

FULL ARTICLE

Rapid and label-free detection and assessment of bacteria by terahertz time-domain spectroscopy

Xiang Yang^{*,1}, Dongshan Wei^{**,2}, Shihan Yan², Yueping Liu¹, Shu Yu¹, Mingkun Zhang², Zhongbo Yang², Xiaoyan Zhu¹, Qing Huang¹, Hong-Liang Cui^{*,2,3}, and Weiling Fu^{*,1}

¹ Department of Laboratory Medicine, Southwest Hospital, Third Military Medical University, Chongqing 400038, China

² Chongqing Key Laboratory of Multi-scale Manufacturing Technology, Chongqing Institute of Green and Intelligent Technology, Chinese Academy of Sciences, Chongqing 400714, China

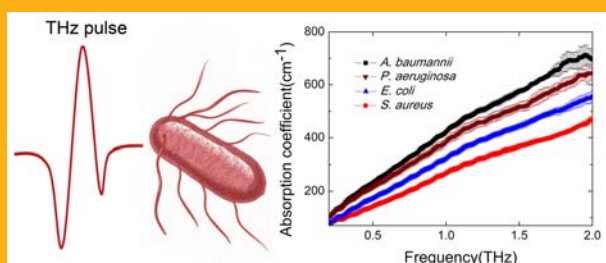
³ College of Instrumentation Science and Electrical Engineering, Jilin University, Changchun, Jilin 130061, China

Received 8 October 2015, revised 8 December 2015, accepted 29 January 2016

Published online 19 February 2016

Key words: bacterial analysis, laboratory medicine, terahertz time-domain spectroscopy, absorption coefficient

Here we demonstrated the potential and applicability of terahertz (THz) spectroscopy to detect four commonly found bacteria in the infectious diseases. Besides the different spectral characteristics between bacterial species, THz absorption differences for living bacteria, dead bacteria and bacterial powder of the same species were also investigated. Our results revealed that small differences in water contents between bacterial cells account for distinct discrepancies of the absorption coefficients, which can be used for bacterial species identification. Furthermore, living and dead bacteria showed different absorption coefficients as a result of their different hydration levels, suggesting that THz spectroscopy can be used to rapidly assess the living state of bacteria under test. Our results clearly demonstrated the ability of THz spectroscopy for time-saving and label-free detection of bacteria with minimal sample preparation, potentially to be utilized for point-of-care tests in the near future.



Schematic representation of bacterial detection by THz spectroscopy. Different bacteria have distinctive absorption coefficients as a result of their different water contents.

1. Introduction

Development of reliable approaches for rapid detection of pathogenic bacteria is important for clinical microbiology. Traditional microbial identification procedure based on phenotypic and biochemical tests after microbial culture is time-consuming. It

usually takes a few days to identify the source of the infection. Without rapid and accurate diagnoses of pathogenic microorganism, patients with infectious diseases have to receive empiric antimicrobial treatment instead of targeted antibiotic prescribing [1]. The overuse of broad-spectrum antibiotics may lead to the alarming mortality associated with limitations in options for effective antibiotic therapy. Conver-

* Corresponding authors: e-mails: hcui@cigit.ac.cn; weiling_fu@126.com

** Author Contributions: X.Y. and DS.W. contributed equally to this work.

sely, knowledge of the specific pathogen would necessarily make a difference in the initial treatment of the patient. It makes excellent sense to develop new techniques with minimal steps for bacterial detection [2, 3]. Despite some emerging technologies that enable the detection of pathogen with new speed for eliminating some time-consuming tasks, they are not without drawbacks. Mass spectrometry and nucleic acid-based amplification technologies like PCR have brought dramatic advances in infectious diseases diagnostics, albeit such approaches are protein-centered and nucleic acid-based analyses, respectively. As such, they fail to differentiate living and dead bacteria as they only confirm the presence of the specific target component instead of a viable organism, whereas the detection of nonviable bacteria is of little significance for making a diagnosis [2]. On the other hand, molecular assays can lead to false-positive results since signals can originate from both viable and dead cells [4]. The integration of multiple technologies will undoubtedly benefit prompt bacterial detection much more than any single technology. It is of great significance to explore complementary detection methods to address the unmet needs.

Optical technologies such as fluorescence and vibrational spectroscopy are probably the most popular solutions for bioanalysis, due to their better sensitivity and selectivity [5, 6]. Terahertz (THz) radiation, generally referred to the frequencies from 0.1 THz to 10 THz, is also called submillimeter wavelength radiation [7]. Terahertz wave, which interrogates characteristic frequency features with length scales spanning tens of micrometers up to several millimeters and reveals time-resolved dynamics on the timescale from sub-picosecond to picosecond, is able to attain unique structural and dynamic information absent in other electromagnetic spectroscopies [8, 9]. This advanced technology has gained widespread attention for its good capability in applications including genetic diagnostics, cancer imaging and biomolecular detection [10–13]. THz radiation can excite low-frequency molecular vibrations from intra/inter-molecular weak interactions including hydrogen bonds, van der Waals and non-bonded (hydrophobic) interactions, etc. When THz wave radiates on the entire bacterial cell, the photon energy of the THz wave largely coincides with the energy levels corresponding to the biomolecular low-frequency motions such as vibration, rotation and translation of the molecular skeleton [14]. Consequently, specific characteristic signals may be found in transmission (absorption) spectra, as a result of the interaction between the THz radiation and low-frequency molecular motions from components of bacteria [14, 15]. Given the variance of cellular constituents, THz wave can be utilized for label-free detection of bacteria on the basis of the specific spectra.

To date, relevant researches on using the THz technologies to detect bacteria mostly focus on spores of *Bacillus* species [16–21]. By using the THz photomixing spectrometer, two distinct signatures at 955 GHz and 1015 GHz were found for *Bacillus thuringiensis* [21], while three distinct signatures at 253 GHz, 418 GHz and 1037 GHz were observed in *Bacillus subtilis* [20]. Using Fourier Transform spectroscopy, different absorption spectra were obtained for living cells of *Escherichia coli* and *Bacillus subtilis* [14]. In addition, the spectral differences between thermally treated cells and untreated cells for *Escherichia coli* and *Bacillus subtilis* also demonstrated the capability of THz technology for rapid assessment of the living state of bacteria under test [14]. These heartening progresses notwithstanding, questions still exist regarding bacterial detection by using THz technologies. First of all, earlier interpretation of THz spectra of bacteria is not clear. Some researchers used molecular dynamics simulations to explore the interaction mechanism between bacteria and THz radiation, and explained the THz absorption spectra of bacteria resulting from vibrational bands within cellular components [22, 23], while other researchers attributed spectral signatures to the presence of optical phonons and electromagnetic interactions of bacterial cells with terahertz radiation [17]. Secondly, the role of the influence of intracellular water plays on the overall THz absorption of bacteria is still not explored at the moment. Furthermore, the aforementioned studies mainly investigated the transmission or absorption spectroscopy, and some related and important physical parameters like refractive index and complex dielectric constants are worth investigating for bacterial detection.

Therefore, the goal of the present study is to investigate the different spectral characteristics between bacterial species of the vegetative bacteria rather than spores (i.e., in their dormant states) to explore the possibility of applying THz spectroscopy to infectious diseases diagnostics. Additionally, spectral characteristics of untreated bacteria were compared with those of thermally treated cells of the same species to explore the spectral difference between living and dead bacteria. Moreover, the role of water in the overall absorption was also investigated by analyzing the THz absorption differences from the living bacteria, dead bacteria and bacterial powder.

2. Experimental

2.1 Sample preparation

Four standard bacterial strains including *Escherichia coli* ATCC 25922, *Staphylococcus aureus* ATCC 25923, *Pseudomonas aeruginosa* ATCC 27853 and

Acinetobacter baumannii ATCC 19606 were purchased from the National Institute for the Control of Pharmaceutical and Biological Products, China. *S. aureus* is a Gram positive bacterium while *E. coli*, *P. aeruginosa* and *A. baumannii* are Gram negative bacteria. Prior to the experiment, the bacteria were grown on blood agar plates (CNA, Pang Tong, Chongqing, China) overnight at 37 °C and bacterial colonies were scraped off of the surface of the plates directly for sample preparation. Part of the bacterial colonies were measured immediately after culture as for living bacteria while another part of the samples were heated in a metal bath at 100 °C for 60 min to prepare dead bacteria. Sterilization efficiency was assessed by inoculating bacterial suspensions to blood agar plates and no bacterial colony was observed after incubation overnight.

Part of the bacterial colonies were put in the freeze dryer (CoolSafe110-4, Labogene, Lyngé, Denmark) overnight working at -110 °C in a vacuum environment to prepare bacterial powder. Then intracellular water was removed from the sample by the direct conversion of the ice (solid phase) to a vapor (vapor phase), without passing through a liquid phase. Subsequently, 0.03 g bacterial powder (bacteria colonies after drying process) were mixed with 0.10 g polyethylene (PE) powder thoroughly and pressed (at 4 tons cm⁻² for 1 minute) into pellets. The diameter of pressed pellets was 15 mm which matches the size of the terahertz light spot and the thickness vary from 0.6 mm to 0.8 mm for different species. After recording bacteria's weight before and after drying process, their individual water contents were obtained. Similarly, water contents of thermally treated bacteria (dead bacteria) were obtained by the freeze dryer. In order to obtain the correct value of bacteria's water content, each kind of bacteria were measured 10 times after identical culture conditions. The obtained water contents of living and dead bacteria of the four species are presented in Table 1. All microbiological procedures were handled safely in a Biosafety Level 1 cabinet (Nuaire, Plymouth, MN, USA).

2.2 THz spectrometer and sample cell

Terahertz spectra measurements were performed using a Picometrix T-ray 5000 fiber-coupled spectro-

meter (Advanced Photonix, Inc., MI, USA) in transmission mode. Figure 1a demonstrates the schematic diagram of the terahertz time-domain spectroscopy (THz-TDS) system. The spectrometer uses femtosecond near-infrared laser pulses and LT-InGaAs photoconductive antenna (PCA) chips to generate and coherently detect the electric field of ultra short THz electromagnetic pulses in the time domain [24].

The sample cell (Figure 1b) employed in this work was modified from a standard Bruker liquid sample cell (model A145, Bruker, Ettlingen, Germany) [25, 26]. Two framing aluminum holders stabilized the demountable cell. The Teflon (PTFE) gasket and neoprene gasket next to the aluminum plates separated the optical window made of PE from the metal surface of the two aluminum plates, respectively. PET double-sided tapes (3M, MN, USA) were tailored into square patches on which one circle with a diameter of 15 mm was hollowed out simultaneously for accommodating the sample. A clean and disposable spacer composed of two PE gaskets was used in every measurement of living and dead bacteria. When sealing the spacer by pasting two PE gaskets together after adding bacterial colonies, excessive bacteria cells can be expelled from any side of the spacer to make sure it is fully filled. After the disposable Secure-Seal spacer was put between the PTFE gasket and neoprene gasket, four gaskets were stabilized by aluminum plates for measurement. With a constant diameter of 15 mm and a thickness of 0.10 mm, different samples were measured and compared in the same volume of the Secure-Seal spacer.

2.3 Measurement

The experimental measurements were conducted at an ambient temperature of 21 ± 0.4 °C, a relative humidity of <2.0%, with the purge of nitrogen gas. THz time-domain waveforms of our samples and the reference signal without a sample were measured under the same experimental condition. For the detection of living and dead bacteria in the fixed sample cell introduced above, the empty spacer was used as a reference to eliminate the background effects. The constant sample thickness 0.10 mm was calculated as the optical path. Pressed pellets were measured after being reinserted in the conventional

Table 1 Water contents^a of bacteria in different living states.

Bacteria	<i>A. baumannii</i> (%)	<i>P. aeruginosa</i> (%)	<i>E. coli</i> (%)	<i>S. aureus</i> (%)
Living bacteria	82.75 ± 0.32	79.32 ± 0.47	77.55 ± 0.51	73.99 ± 0.44
Dead bacteria	77.31 ± 1.91	73.01 ± 1.39	70.39 ± 1.01	66.37 ± 0.97

^a Water contents were shown as mean ± standard deviation (*N* = 10).

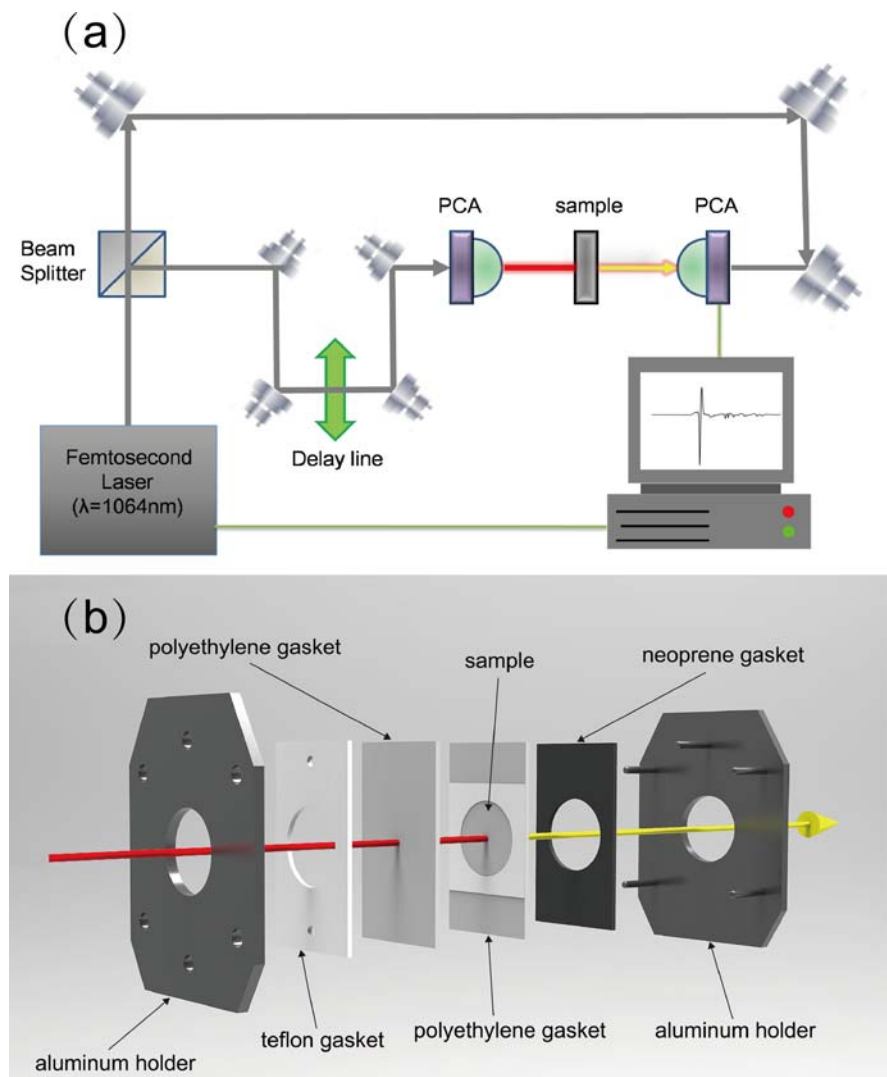


Figure 1 Schematic diagram of the THz Spectrometer: setup of the terahertz time-domain spectroscopy system **(a)** and the stereo diagram showing the sample cell **(b)**. After the disposable PE gaskets loaded with bacterial cells were put in the sample cell, spectral characteristics of bacteria can be obtained by Fourier transform of the measured time-domain signals containing amplitude and phase information.

sample holder. Considering PE powder as ideal for preparing mixtures with the substances to be analyzed [27], the pure PE sample pellet was measured to obtain the reference upon which every pressed pellet was compared. The frequency-domain spectra of measured signals are obtained by Fourier transform (FT). The effective frequency region is 0.2 THz to 2.0 THz with this THz-TDS setup. Spectral frequency resolution of the spectrometer is 12.5 GHz. Due to bacteria's viable state, every species of bacteria was measured in 5 samples to minimize the heterogeneities in the sample. The same experiment was repeated on another day in order to eliminate the influences of humidity and instrument performance.

2.4 Data analysis

The THz optical refractive index of the bacteria is calculated using standard algorithm [28, 29],

$$n(f) = \frac{|\varphi_s(f) - \varphi_{ref}(f)| c}{2\pi f d} + 1 \quad (1)$$

where $\varphi_s(f)$, $\varphi_{ref}(f)$ are the phase angles of the Fourier transforms of the power transmissions of the bacterial sample, I_s , and the power transmissions of the reference (the blank sample cell), I_{ref} , respectively, and c is the light speed and f is the frequency. d is the optical path the THz pulse of radiation passing through samples before being detected. To derive the dielectric constant, the extinction coefficient, $\kappa(f)$, is obtained as,

$$\kappa(f) = \ln \left[\frac{4n(f)}{\rho(f) [n(f) + 1]^2} \right] \frac{c}{2\pi f d} \quad (2)$$

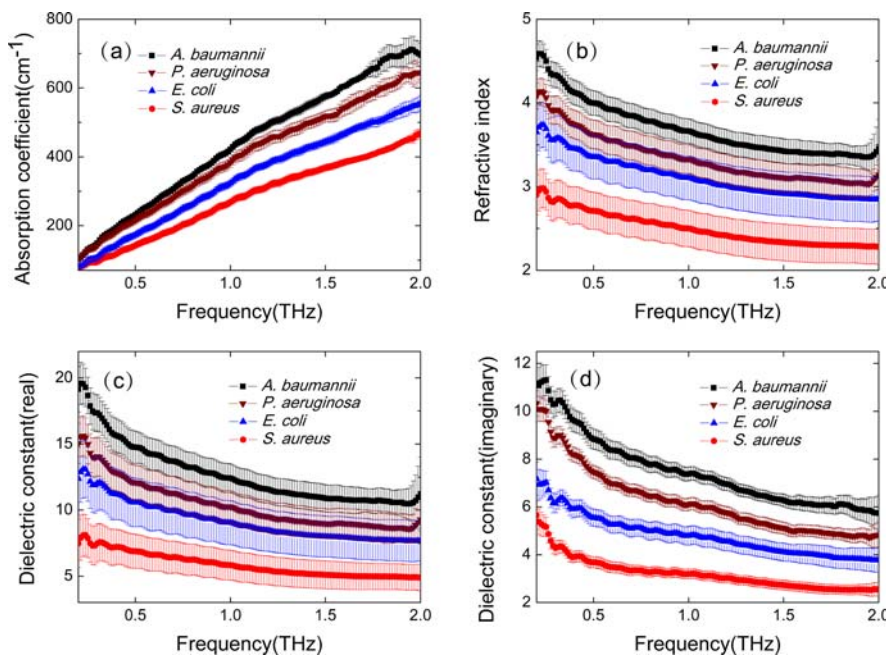


Figure 2 Bacterial species-specific THz optical constants: absorption coefficient (a); refractive index (b); real part of the dielectric constant (c) and imaginary part of the dielectric constant (d). Error bars indicate the standard deviation ($N = 10$).

where $\rho(f)$ is the amplitude ratio of the Fourier transforms of I_s and I_{ref} . The absorption coefficient of bacteria, α , is deducted as

$$\alpha(f) = \frac{4\pi f k(f)}{c} \quad (3)$$

and the complex dielectric constant, $\hat{\epsilon}(f)$, is expressed as

$$\hat{\epsilon}(f) = [n(f) - ik(f)]^2 = \epsilon_1 - i\epsilon_2 \quad (4)$$

where ϵ_1 and ϵ_2 are the real and imaginary parts of the complex dielectric constant, respectively.

Group differences of absorption coefficients between living bacteria, dead bacteria and bacterial powder were statistically analyzed by performing one-way analysis of variance (ANOVA) with a *post-hoc* test, and the statistical differences between two groups were determined by the least significant difference (LSD) test. The statistical significance was set at $P < 0.05$.

3. Results and discussion

3.1 THz optical constants of bacteria

Figure 2 shows the absorption coefficient α , refractive index n , real part of the dielectric constant ϵ_1 and imaginary part of the dielectric constant ϵ_2 for four species of living bacteria in the 0.2 THz to 2.0 THz range. In order to compare the different parameters between bacterial species, statistics error

bars calculated from the population standard deviation were used after smoothing curves by adjacent averaging of the nearest 15 data points. A more rigorous curve smoothing method is to use an optimal algorithm [30] to remove the interfering Fabry-Perot oscillations resulting from multiple internal reflections between the medium interfaces, but the convergence of the optimal algorithm is poor because of the multilayer structure of the sample cell we used. Hence we chose a simple adjacent averaging method to smooth the data. Despite the overlapped error bars in the THz spectra of refractive index and real dielectric constant, there were still significant differences for both absorption coefficient and imaginary dielectric constant. Considering the fact that the dielectric constants are calculated from absorption coefficient and refractive index, we directly chose the absorption coefficient for bacterial species identification by THz spectroscopy. In contrast, differences of absorption coefficients seemed to be much smaller for bacterial powder. It was difficult to distinguish the differences between *P. aeruginosa*, *E. coli* and *A. baumannii*, as shown in Figure 3. Comparing Figures 2a to 3, we found that absorption coefficients of living bacteria were around 300 cm^{-1} at 1.0 THz while the corresponding values were only about 13 cm^{-1} for bacterial powder, which were at least an order of magnitude lower than the former. Moreover, the orders of absorption coefficient values were not identical for two different states of bacteria. For living bacteria, the absorption coefficients were *A. baumannii* > *P. aeruginosa* > *E. coli* > *S. aureus*, while values for bacterial powder were approximately in the order: *S. aureus* > *E. coli* > *P. aeruginosa* > *A. baumannii*. In other words, living cells of

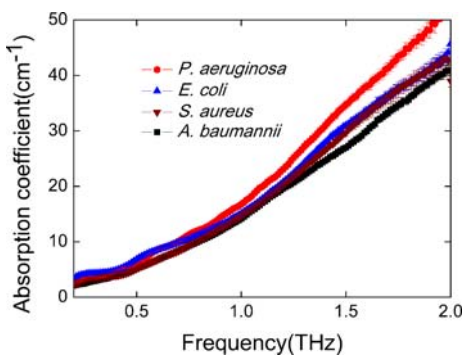


Figure 3 Absorption coefficients for bacterial powder. They were at least an order of magnitude lower than that of living bacteria, indicating that the intracellular water contributed greatly to the overall absorption.

S. aureus had the lowest absorption in the THz range among four kinds of bacteria, even though the dry bacterial components were more absorbing than *E. coli*, *P. aeruginosa* and *A. baumannii* after intracellular water was removed. Due to the strong absorption of water in the THz frequency range [10], we think the intracellular water should contribute greatly to the overall absorption. The differences in quantity and the inconsistency in the ordering demonstrated that the influence of water absorption seemed to be greater than that of dry bacterial components.

No significant absorption peak was observed for all of the four living bacteria in the THz absorption spectra. Two reasons may account for this phenomenon. Firstly, the samples we detected were vegetative bacteria, which were provided with significantly higher intracellular water contents than spores [31], and large density of overlapping states of absorption bands might obscure vibrational resonances, especially for thick samples in this work (i.e., 100 µm). Secondly, the spectral resolution of the instrument in this study is relatively poor compared to others, e.g., photomixing THz spectrometers (12.5 GHz vs. <1 GHz) [32]. Studies by Globus et al. have shown that rich characteristic spectra were observed for cells of *Escherichia coli* and *Bacillus subtilis* using the Fourier Transform spectroscopy at the very low measurement temperature of 1.7 K [14]. At room temperature, the rich characteristic spectra were completely washed out due to instantaneous conformational changes of biomolecules, strong thermal broadening, and the significant THz absorption of water molecules in the bacterial cells [29]. Although no absorption peak was demonstrated, THz spectroscopy is still capable of characterizing different bacteria species according to the obvious value differences in absorption coefficients.

3.2 THz absorption by intracellular water

Water is a proper intracellular solvent and medium for various chemical reactions. Intracellular water molecules adjacent to and interacting strongly with biomolecular surfaces are called hydration water while the remaining intracellular water molecules are thought to constitute bulk water [33]. To gain further insight into the influence of water on THz absorption, we used a simple two-component model [34], $\alpha_{\text{est}} = \alpha_{\text{H}_2\text{O}} \cdot x_{\text{H}_2\text{O}} + \alpha_{\text{BP}} \cdot x_{\text{BP}}$, where $\alpha_{\text{H}_2\text{O}}$ and α_{BP} are absorption coefficients of bulk water and bacterial powder while $x_{\text{H}_2\text{O}}$ and x_{BP} are their percentage compositions, respectively. Considering the comparability between the estimated and measured absorption coefficients, the absorption coefficient of bulk water was measured in the aforementioned sample cell. This two-component model gives the estimated absorption coefficient α_{est} by adding up the two parts of contributions from bulk water and bacterial powder, assuming that all intracellular water is bulk water. Figure 4 shows the comparison between the measured value and the estimated value of the absorption coefficient for *E. coli*. It is obvious that not only the experimental value of the absorption coefficient was always larger than the estimated value of *E. coli* over the measured THz range, but also the two curves were inconsistent in shape. The discrepancy clearly proves that hydration water with dynamical properties is much more absorbing than bulk water and the overall absorption is not the simple superposition of bulk water molecules and dry matter composition. Both the dynamics of hydration shells around the surface of biomacromolecules and structural fluctuations of water molecules contribute greatly to the THz absorption [25, 26]. In theory, salvation dynamics studies [35] revealed that the dynamic response time of hydration water is more than an order of magnitude longer than that of bulk water (i.e., ~ps). Consequently, THz-TDS spectro-

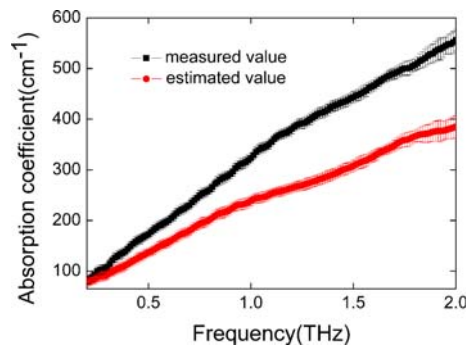


Figure 4 Comparison between the true value and estimated value of absorption coefficients for *E. coli*. The difference illuminates that hydration water molecules contribute greatly to the overall absorption.

scopy enables time-resolved investigation of these hydration dynamical processes since they are on the same timescale. Due to the strong absorption of water in the THz range, the small differences of water contents were enough to be manifested as distinct discrepancies of the overall absorption for bacterial cells, which were used for bacterial species identification in this work.

The present study is designed to search for spectral differences between bacterial species. We assign the quite minute residual moisture between cells (the intercellular water) after culture to the intrinsic cellular components of bacteria (i.e., bacterial mucilage), and consider all the water molecules in the samples as intracellular water. Given the purity and homogeneity of the samples, we deem that any difference in our measurement results should be attributable to the intrinsic optical characteristics of the bacterial species. Considering that the tiny amount of intercellular water replaced the “unfreezable” water in the cellular systems during the drying process which is not calculated, our measured intracellular water content range of 74~83 wt% for the four living bacteria, as shown in Table 1, is consistent with the previous results for living cells [33, 36]. More interestingly, the order of the intracellular water content is consistent with that of the absorption coefficients for living bacteria. It further attests that the intracellular water content, including hydration water and bulk water, should be the dominant factor contributing to the overall THz absorption. Previous work has also demonstrated spectroscopic features of bacteria originating from the combination of low frequency vibrational modes within cell components, with significant contribution from the DNA [14]. In addition, by comparing the transmission spectra, some features of *Bacillus* spores are in common with dipicolinic acid [18, 19], which is a major constituent of the spore coating. However, our results showed that, for living bacteria, intracellular water is undoubtedly the dominant factor contributing to the overall absorption spectra.

3.3 THz absorption of bacteria in different living states

In addition to bacterial species-specific optical constants, it is also interesting to compare the THz spectral differences for bacteria of the same species in different states. Figure 5a presents the comparison of the absorption coefficients for *S. aureus*: living bacteria, dead bacteria and bacterial powder. The curves for living bacteria and dead bacteria were similar in shape but obvious value differences can be seen in the measured THz range. Drastically different was the bacterial powder, of which the absorp-

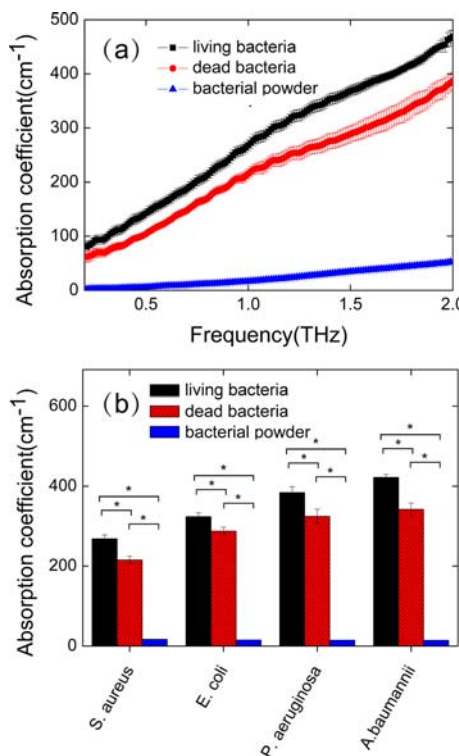


Figure 5 THz absorption differences for bacteria in different living states. (a) Comparison of absorption coefficients for living bacteria, dead bacteria and bacterial powder of *S. aureus*. (b) Different values of absorption coefficients at 1.0 THz for the four bacterial species, respectively. All data are shown as the mean \pm standard deviation. * $P < 0.05$. One-way analysis of variance (ANOVA) with a post-hoc test was performed, and the statistical differences between two groups were determined by the least significant difference (LSD) test.

tion coefficients were at least an order of magnitude lower than that of both the living and the dead bacterial cells, after the intracellular water was removed. To clarify the differences, we compared the values of absorption coefficients at 1.0 THz for the four bacterial species, respectively, as illustrated in Figure 5b. The results proved that not only the living and the dead bacteria were markedly more absorbing than the bacterial powder but also the absorption differences for the living and the dead bacteria of the same species were statistically significant. The discrepancies may be explained in terms of the changes of frequency modes as a result of irreversible transformation of cell components, including intracellular protein and nucleic acids [14]. In addition to structural injury, loss of cellular lipopolysaccharide and leakage of intracellular substances due to disintegration of the membrane structure might also be responsible [37]. Since water is a vital indicator for metabolic activities, living and dead bacteria have different intracellular water contents (Table 1),

and the ratios of bulk water and hydration water, which can be detected by THz spectroscopy and shown as different curves in the absorption coefficient spectra. In addition, a previous study [32] demonstrated that *Bacillus thuringiensis* in log phase and in late stationary phase had slightly different attenuation signatures in the terahertz region, due to their different hydration levels, which was in line with our results.

Here we must acknowledge the defect of ignoring several other aspects of the THz radiation propagating through the sample cell when calculating absorption values for living and dead bacteria. Due to the existence of the two PE gaskets, scattering loss was inevitable and the calculated absorption coefficients were most likely to be overestimated. But since all these samples were prepared in the same sample thickness and measured in the same specification of spacers, the essential value differences between bacterial species should not be affected. Bacterial powder was measured in pellets so it seems inappropriate to directly compare the absorption coefficients of living bacteria to bacterial powder because radiation loss should be different for these distinct media. However, the obvious value differences in Figures 4 and 5 have clearly demonstrated the essential distinctions, which cannot be explained by the radiation loss such as scattering alone. This technology is at an early stage of development and much more work needs to be done to demonstrate the selectivity besides the four chosen species. Nonetheless, it is worth noting that this method requires only two steps to identify pathogenic microorganism: loading bacterial colonies to the sample cell and measuring its time-domain signal to calculate the absorption coefficient, which only takes 1–2 minutes after microbial culture. The simplicity enables its utilization access to minimally trained personnel in diverse healthcare settings. As shown in Table 1, bacteria of the same species possess relatively constant water content under identical culture conditions (standard deviation <1% for living bacteria). Therefore, a systematic collection of spectral characteristics to develop reference spectral library can be completed with the quantification of water contents under identical culture conditions for some commonly interested target bacteria. Akin to spectral profiles based on mass-to-charge ratios for mass spectroscopy, after building the bacterial THz spectral database composed of absorption coefficients delineated by their water contents, terahertz technology can be used for detecting an unknown bacterium in remote areas where resources is limited. Furthermore, besides its rapidness and simplicity, THz spectroscopy has the ability of assessing the living state of bacteria under test (i.e., distinguish between living and dead bacteria), which is a significant advantage to the existing tools. The recently reported compact and portable

THz spectrometer(180 in³ and 4.2 lbs) [9], considerably smaller and lighter than conventional THz systems, can be used to detect biological tissues with quite good performance, showing its potential for rapid assessment of infectious diseases in medical evacuation aircraft or battlefield hospitals [38]. Moreover, nano- and micro-structures such as the discontinuity effect in sub-wavelength periodic slit arrays and gap structures in metamaterials can be used to increase the coupling of THz radiation to substances under test due to the strong local electromagnetic field enhancement, thus enabling detection of extremely small amounts of sample [39–41]. It has been reported that Gram-positive and Gram-negative bacteria have different dielectric response in the terahertz region because of their different structures and chemical environment properties [42]. After integrating the periodic slit arrays in a sample cell, only trace amounts of bacterial cells are required to be detected, which greatly improves the detection sensitivity.

4. Conclusion

Our results illustrated that the small differences of water contents can be characterized as distinct discrepancies of the absorption coefficients by THz spectroscopy. Moreover, living and dead bacteria of the same species also showed different absorption coefficients as a result of their different hydration levels. By filling some critical gaps at the present stage, this novel label-free, cost-effective and rapid detection and assessment ability of the living state will significantly contribute to the acquisition of a more complete picture of bacterial identification. The goal at the present stage is to employ a signal amplification technique to extract the signals of target bacteria, which is underway in our laboratory and will be addressed in an upcoming publication.

Acknowledgements This work was partially supported by the National Basic Research Program of China (No. 2015CB755400), the National Natural Science Foundation of China (No. 81430054), the Military Medical Pre-research Funds of The Third Military Medical University (No. SWH2013JS05) and the Physics and Biomedical Cross Laboratory Incubator Funds (No. WSS-2014-08).

References

- [1] A. M. Caliendo, D. N. Gilbert, C. C. Ginocchio, K. E. Hanson, L. May, T. C. Quinn, F. C. Tenover, D. Allard, A. J. Blaschke, R. A. Bonomo, K. C. Carroll, M. J. Ferraro, L. R. Hirschhorn, W. P. Joseph, T. Karchmer, A. T. MacIntyre, L. B. Reller, and A. F. Jackson, Clin. Infect. Dis. **573**, S139–S170 (2013).

- [2] B. W. Buchan and N. A. Ledeboer, *Clin. Microbiol. Rev.* **27**, 783–822 (2014).
- [3] H. Schulze, G. Giraud, J. Crain, and T. T. Bachmann, *J. Biophotonics* **2**, 199–211 (2009).
- [4] K. L. Josephson, C. P. Gerba, and I. L. Pepper, *Appl. Environ. Microbiol.* **59**, 3513–3515 (1993).
- [5] O. Lazcka, F. J. Del Campo, and F. X. Munoz, *Biosens. Bioelectron.* **22**, 1205–1217 (2007).
- [6] C. Sousa, F. Gross, L. Meirinhos-Soares, L. Peixe, and J. Lopes, *J. Biophotonics* **7**, 287–294 (2014).
- [7] A. Abbas, A. Treizebre, P. Supiot, N.-E. Bourzgui, D. Guillochon, D. Vercaigne-Marko, and B. Bocquet, *Biosens. Bioelectron.* **25**, 154–160 (2009).
- [8] D. F. Plusquellec, K. Siegrist, E. J. Heilweil, and O. Esenturk, *Chemphyschem* **8**, 2412–2431 (2007).
- [9] G. J. Wilmink, B. L. Ibey, T. Tongue, B. Schulkin, N. Laman, X. G. Peralta, C. C. Roth, C. Z. Cerna, B. D. Rivest, J. E. Grundt, and W. P. Roach, *J. Biomed. Opt.* **16** 047006 (2011).
- [10] M. Tonouchi, *Nat Photonics* **1**, 97–105 (2007).
- [11] A. Arora, Q. L. Trung, M. Krueger, Y. J. Kim, C.-H. Nam, A. Manz, and M. Havenith, *Analyst* **137**, 575–579 (2012).
- [12] C. Wang, J. Gong, Q. Xing, Y. Li, F. Liu, X. Zhao, L. Chai, C. Wang, and A. M. Zheltikov, *J. Biophotonics* **3**, 641–645 (2010).
- [13] C. S. Joseph, R. Patel, V. A. Neel, R. H. Giles, and A. N. Yaroslavsky, *J. Biophotonics* **7**, 295–303 (2014).
- [14] T. Globus, T. Dorofeeva, I. Sizov, B. Gelmont, M. Lvovska, T. Khromova, O. Chertihin, and Y. Koryakina, *Am. J. Biomed. Eng* **2**, 143–154 (2012).
- [15] T. Globus, A. M. Moyer, B. Gelmont, T. Khromova, M. I. Lvovska, I. Sizov, and J. Ferrance, *IEEE SENS J* **13**, 72–79 (2013).
- [16] T. J. Johnson, N. B. Valentine, and S. W. Sharpe, *Chem. Phys. Lett.* **403**, 152–157 (2005).
- [17] E. R. Brown, T. B. Khromova, T. Globus, D. L. Wooldard, J. O. Jensen, and A. Majewski, *IEEE SENS J* **6**, 1076–1083 (2006).
- [18] B. L. Yu, A. Alimova, A. Katz, and R. R. Alfano, THz absorption spectrum of *Bacillus subtilis* spores, in *Proc. SPIE 5727, Terahertz and Gigahertz Electronics and Photonics IV* (2005).
- [19] M. J. Fitch, C. Dodson, D. S. Ziomek, and R. Osiander, Time-domain terahertz spectroscopy of bioagent simulants, in *Proc. SPIE 5584, Chemical and Biological Standoff Detection II* (2004).
- [20] E. R. Brown, J. E. Bjarnason, T. L. J. Chan, A. W. M. Lee, and M. A. Celis, *Appl. Phys. Lett.* **84**, 3438–3440 (2004).
- [21] W. Zhang, E. R. Brown, L. Viveros, K. P. Burris, and C. N. Stewart, Jr., *J. Biophotonics* **7**, 818–824 (2014).
- [22] T. Globus, I. Sizov, and B. Gelmont, *Adv Biosci Biotechnol.* **04**, 493–503 (2013).
- [23] N. Alijabbari, Y. Chen, I. Sizov, T. Globus, and B. Gelmont, *J. Mol. Model.* **18**, 2209–2218 (2012).
- [24] J. D. Buron, D. H. Petersen, P. Boggild, D. G. Cooke, M. Hilke, J. Sun, E. Whiteway, P. F. Nielsen, O. Hansen, A. Yurgens, and P. U. Jepsen, *Nano Lett.* **12**, 5074–5081 (2012).
- [25] B. Born, S. J. Kim, S. Ebbinghaus, M. Gruebele, and M. Havenith, *Faraday Discuss.* **141**, 161–173 (2009).
- [26] B. Born, H. Weingaertner, E. Bruendermann, and M. Havenith, *J. Am. Chem. Soc.* **131**, 3752–3755 (2009).
- [27] A. Redo-Sanchez, G. Salvatella, R. Galceran, E. Rodolos, J. A. Garcia-Reguero, M. Castellari, and J. Tejada, *Analyst* **136**, 1733–1738 (2011).
- [28] J. T. Kindt and C. A. Schmuttenmaer, *J. Phys. Chem.* **100**, 10373–10379 (1996).
- [29] F. Bernd, H. Matthias, H. Hanspeter, W. Rafal, R. Frank, K. O. Thomas, K. Martin, and J. Peter, *Opt. Express* **13**, 5205–5215 (2005).
- [30] M. Scheller, *J. Infrared. Millim. Te* **35**, 638–648 (2014).
- [31] B. S. Henry and C. A. Friedman, *J. Bacteriol.* **33**, 323–329 (1937).
- [32] W. Zhang, E. R. Brown, L. Viveros, K. P. Burris, and C. N. Stewart, Jr., *J. Biophotonics* **7**, 818–824 (2014).
- [33] R. Cooke and I. D. Kuntz, *Annu. Rev. Biophys. Bioeng.* **3**, 95–126 (1974).
- [34] Y. Sun, Y. Zhang, and E. Pickwell-Macpherson, *Bioophys J* **100**, 225–231 (2011).
- [35] S. K. Pal, J. Peon, and A. H. Zewail, *Proc Natl Acad Sci U S A* **99**, 1763–1768 (2002).
- [36] F. Feijo Delgado, N. Cermak, V. C. Hecht, S. Son, Y. Li, S. M. Knudsen, S. Olcum, J. M. Higgins, J. Chen, W. H. Grover, and S. R. Manalis, *PLoS One* **8**, e67590 (2013).
- [37] A. D. Russell and D. Harries, *Appl. Microbiol.* **15**, 407–410 (1967).
- [38] P. Zhao, S. Ragam, Y. J. Ding, and I. B. Zotova, *Opt. Lett.* **35**, 3979–3981 (2010).
- [39] H.-R. Park, K. J. Ahn, S. Han, Y.-M. Bahk, N. Park, and D.-S. Kim, *Nano Lett.* **13**, 1782–1786 (2013).
- [40] S. J. Park, J. T. Hong, S. J. Choi, H. S. Kim, W. K. Park, S. T. Han, J. Y. Park, S. Lee, D. S. Kim, and Y. H. Ahn, *Sci. Rep.* **4**, 7 (2014).
- [41] R. Parthasarathy, A. Bykhovski, B. Gelmont, T. Globus, N. Swami, and D. Woolard, *Phys. Rev. Lett.* **98**, 153906 (2007).
- [42] A. Berrier, M. C. Schaafsma, G. Nonglaton, J. Bergquist, and J. G. Rivas, *Biomed. Opt. Express* **3**, 2937–2949 (2012).